Journal of Magnetic Resonance 204 (2010) 91–98

Contents lists available at ScienceDirect

Journal of Magnetic Resonance

journal homepage: www.elsevier.com/locate/jmr

In vivo 1D and 2D correlation MR spectroscopy of the soleus muscle at 7T

Saadallah Ramadan [a,*], Eva-Maria Ratai [b], Lawrence L. Wald [b], Carolyn E. Mountford [a]

[a] *Centre for Clinical Spectroscopy, Department of Radiology, Brigham and Women's Hospital, Harvard Medical School, 4 Blackfan St., H.I.M., 8th Floor, Boston, MA 02115, USA*
[b] *Athinoula A. Martinos Center for Biomedical Imaging, Department of Radiology, Massachusetts General Hospital, 149 Thirteenth Street, Charlestown, MA 02129, USA*

ARTICLE INFO

Article history:
Received 26 November 2009
Revised 7 January 2010
Available online 12 February 2010

Keywords:
MR spectroscopy
L-COSY
7 Tesla
Soleus muscle
In vivo
Human
Intra-myocellular and extramyocellular lipids

ABSTRACT

Aim: This study aims to (1) undertake and analyse 1D and 2D MR correlation spectroscopy from human soleus muscle *in vivo* at 7T, and (2) determine T1 and T2 relaxation time constants at 7T field strength due to their importance in sequence design and spectral quantitation.
Method: Six healthy, male volunteers were consented and scanned on a 7T whole-body scanner (Siemens AG, Erlangen, Germany). Experiments were undertaken using a 28 cm diameter detunable birdcage coil for signal excitation and an 8.5 cm diameter surface coil for signal reception. The relaxation time constants, T1 and T2 were recorded using a STEAM sequence, using the 'progressive saturation' method for the T1 and multiple echo times for T2. The 2D L-Correlated SpectroscopY (L-COSY) method was employed with 64 increments (0.4 ms increment size) and eight averages per scan, with a total time of 17 min.
Results: T1 and T2 values for the metabolites of interest were determined. The L-COSY spectra obtained from the soleus muscle provided information on lipid content and chemical structure not available, *in vivo*, at lower field strengths. All molecular fragments within multiple lipid compartments were chemically shifted by 0.20–0.26 ppm at this field strength. 1D and 2D L-COSY spectra were assigned and proton connectivities were confirmed with the 2D method.
Conclusion: In vivo 1D and 2D spectroscopic examination of muscle can be successfully recorded at 7T and is now available to assess lipid alterations as well as other metabolites present with disease. T1 and T2 values were also determined in soleus muscle of male healthy volunteers.

1. Introduction

Two-Dimensional MR spectroscopy, first reported by Jeener [1,2] as a simple two-pulse sequence and known as the Correlated SpectroscopY (COSY) experiment, has proven invaluable in many disciplines. Unlike stable chemical compounds and relatively stable proteins, cultured cells and tissue biopsy specimens have a limited experimental time due to metabolic degradation. This changed the perspective of data acquisition and analysis for 2D MR data sets. The 2D COSY method was first applied to cells in 1984 [3] and then to tissues in 1988 [4].

It was demonstrated that both viable cells and tissues give rise to a plethora of resonances, up to 60 different chemical species all of which can alter simultaneously with the onset and development of disease [5]. It was, however, realized that the study of cells and tissues involved a detailed and complex inter-relationship of biochemical pathways that with appropriate clinical and pathological correlation provided, biochemical, diagnostic and prognostic information [6–14]. The wide range of molecules with equally diverse T1 and T2 relaxation values meant that any one 2D data set needed to be post processed using different mathematical criteria in order to inspect all molecules active on the MR timescale [15].

The literature on 2D MRS of biopsies paved the way for *in vivo* 2D studies on humans. The first COSY studies were undertaken on the brain [16] at a 2T field strength with a voxel size of 240 cm^3 and total experimental time of 102 min. The resultant 2D spectra were broad and most cross-peaks were weak and overlapped. Whilst these early results proved that 2D data could be accrued *in vivo*, it also became clear that the spectral dispersion obtained at higher fields is important for diagnostic purposes.

With the introduction of higher field magnets for clinical usage i.e. 3T and above, the utilization of *in vivo* 2D spectroscopy became an option for the interrogation of biochemistry of disease and could assist with unambiguous resonance assignment. The higher the field strength, the greater the potential for improved SNR, spectral resolution and reduced spectral acquisition time [17].

Our objective here was to firstly evaluate the chemical information available from the 2D L-COSY [18] recorded from human soleus muscle, *in vivo* at 7T, and to ascertain if this technology could provide information on the pools of lipids and their contents. Localized MRS has been applied successfully, by others, to human

* Corresponding author. Fax: +1 617 525 7533.
E-mail address: saad.ramadan@gmail.com (S. Ramadan).

1090-7807/$ - see front matter © 2010 Elsevier Inc. All rights reserved.
doi:10.1016/j.jmr.2010.02.008

skeletal muscle *in vivo* where two lipid pools, referred to as intramyocellular lipids (IMCL) and extramyocellular lipids (EMCL) [19–22], were reported. It was proposed that the resonances from the lipids in the muscle spectra were seen as two signals due to the geometrical arrangement and anisotropic susceptibility of these lipid compartments [19].

Secondly we aimed to measure the relaxation characteristics of human soleus muscle at 7T. Relaxation measurements can be challenging at high fields as the evolution of J-coupled species is TE dependent and can complicate spectral line shapes. Such measurements are necessary for the design of pulse sequences. Despite the reports of relaxation properties for soleus and tibialis anterior muscles (3T) [23], soleus muscle (1.5T) [20], skeletal muscle (1 and 2.4T) [24], soleus, tibialis posterior and tibialis anterior (4T) [25], tibialis anterior muscle (7T) [26], the literature to date has failed to provide a comprehensive report of all T1 and T2 values for the soleus muscle.

We report here the complete relaxation properties (T1 and T2 values) for the 1D spectra from the soleus muscle of healthy volunteers at 7T, and the chemistry recorded *in vivo* using the 2D L-COSY method which provides better spectral dispersion and more certainty in resonance assignment.

2. Experimental

2.1. Volunteers

Apparently healthy male volunteers ($n = 6$, mean age = 33 ± 9.3 years), taking no medication, participated in this study. An all male cohort was chosen to avoid any sources of error due to the prior claim that the degree of unsaturation within IMCL and EMCL was lower in female subjects than male subjects, and that total lipid content in females was higher than in males [27]. To ensure reproducibility of measurements, the spectroscopic voxel was located in superior third of the soleus muscle. Informed consent was obtained from all participants. All subjects were supinely positioned (feet first) with their right leg inside a transmit coil. To improve separation between IMCL and EMCL and retain residual dipolar couplings, care was taken to position the leg parallel to the Bo field [19,28]. This study was approved by the local institutional review board.

2.2. MR imaging and spectroscopy

Experiments were performed on a 7T whole-body scanner (Siemens AG, Erlangen, Germany, software version VB15A), operating at a proton resonance frequency of 297.18 MHz, using and a 28 cm diameter detunable birdcage coil for signal excitation. Magnetic resonance imaging (MRI) and spectroscopy (MRS) in muscle were performed using an 8.5 cm diameter surface coil for signal reception.

2.2.1. Muscle MRI

Prior to the spectroscopy sequences being undertaken, FLASH 2D gradient echo images were acquired in all three dimension using the following parameters: TE/TR = 5/30 ms, FOV = 200 × 200 mm^2, matrix = 512 × 512, slice thickness = 5 mm, inter-slice spacing = 6 mm, and a flip angle = 10°.

2.2.2. T1 spectroscopic measurements

T1 was measured using the "progressive saturation" method [29–32]. A voxel size of 15 × 15 × 20 mm^3, and a TE of a stimulated echo acquisition mode pulse sequence (STEAM) [33,34] was set to 20 ms, mixing time to 10 ms, while TR was set to 430, 530, 650, 750, 950, 1500, 2000, 3000, 4000, 6000, 7000 ms, with a constant number of 16 averages, acquisition duration of 170 ms, four dummy preparation scans, 512 points per echo were acquired, a bandwidth of 3 kHz, RF offset frequency was set to 1.7 ppm lower than water frequency (i.e. on creatine methyl group), and water suppression routine 'WET' was activated [35]. 'WET' method is made out of three shaped frequency selective RF pulses, each followed by a spoiler gradient pulse aligned along orthogonal orientations. 'WET' water suppression technique was used for all spectroscopic experiments were water suppression is required. Raw data was zero-filled to 1.5 k before FT and was then manually phased. We made sure that at all times TE was much smaller TR so that progressive saturation method could be reliably implemented [32]. T1 was calculated as the slope of a straight line obtained by plotting – TR versus $\mathrm{Ln}\left(1-\frac{S}{S_o}\right)$, where S and S_o are resonance integrals at individual TR values and maximum TR values, respectively. To measure T1 value of water, the number of averages was dropped to four, water suppression was disabled, and all other parameters were kept the same. Spectral raw data processing and fitting were done with JMRUI [36], whereas T1 and error propagation were done with Mathematica [37].

2.2.3. T2 spectroscopic measurements

A series of STEAM 1D experiments, using the same voxel size and positioning as described above, were acquired at TE values of 50, 100, 150 and 200 ms and TR set to 7s, spectral width 3 kHz, 512 acquired points, 170 ms acquisition duration, four dummy preparation scans, 16 averages per TE value, RF offset frequency was set to 1.7 ppm lower than water frequency (i.e. on creatine methyl), and water suppression was activated ('WET' technique) [35]. In some subjects, data points TE = 250 and 300 ms were also acquired, but T2 results were not affected by these additional points, and thus were omitted for remaining subjects. Raw data was zero-filled up to 1.5 k before FT and was then manually phased. T2 was calculated as the slope of a straight line obtained by plotting TE versus Ln(S), where S is resonance integral at different TE values. Multi-exponential behavior of T2, i.e. presence of multiple compartments, was tested by multi-exponential fitting of data acquired at above TE values as well as TE values of 250 and 300 ms. To measure T2 value of water, the number of averages was dropped to four, water suppression was disabled, and all other parameters were kept the same. Spectral raw data processing and fitting were undertaken using JMRUI [36], whereas T1 and error propagation calculations were undertaken using Mathematica (Wolfram, version 6) [37].

2.2.4. L-COSY measurements

The same voxel as was used for T1 and T2 measurements was also used for L-COSY. The L-COSY sequence was applied with a TE (initial) of 30 ms, TR of 2s, eight averages per increment, spectral width in F2 was 4000 Hz, t1 increment size of 0.4 ms, indirect spectral width used was 2500 Hz and the number of increments was 64. The "WET" water suppression method [35] was applied before the acquisition sequence. The L-COSY acquisition time was 17 min. Data processing was done using Felix software package [38], using the following processing parameters used were: F2 domain (skewed sine-squared window, 2048 points, magnitude), F1 domain (sine-squared window, linear prediction to 128 points, zero-filling to 512 points, magnitude). The total creatine methyl resonance at 3.02 ppm was used as an internal chemical shift reference in F1 and F2 [20]. Specific absorption rate (SAR) was within acceptable limits at all times.

2.2.5. Statistical analysis

T1, T2 and L-COSY data were acquired from a single subject two times to ensure intra-subject reproducibility. Inter-subject vari-

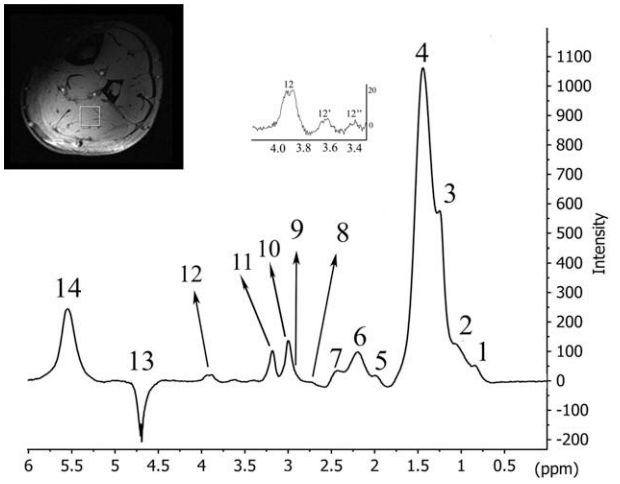

Fig. 1. A localized 1D spectrum acquired from soleus muscle. Axial image of "a" of human soleus muscle from a 38 year old volunteer is shown inset and the voxel position from where the data was collected. About 3.3–4.3 ppm spectral region is expanded to show detail. See Table 1 for assignments. Acquisition parameters are: spectral width; 4000 Hz, vector size; 2048 points, voxel size of $6 \times 6 \times \times 35$ mm^3, number of averages; 8, and repetition time; 2000 ms. The "WET" water suppression method [35] was applied before the acquisition sequence. The 1D spectrum was Fourier transformed after zero-filling to 4096 points and applying an exponential window function in MestReNova program [52].

ability of measurable constants and ratios was evaluated by means of variance analysis. JMP software (SAS Institute, Cary, NC, USA) was used for statistical analysis. All values are reported as mean (standard deviation, SD).

3. Results

A typical 1D MRS result is shown in Fig. 1. Resonances in 1D spectrum (Fig. 1) were identified, assigned and listed in Table 1.

A typical 2D L-COSY spectrum recorded during this study is shown in Fig. 2 and labeled as described in May et al. [14] and summarized in Ramadan et al. [39]. A vertical ridge of noise (t1-noise) at ~1.6 ppm was observed in most L-COSY spectra when vertical display is very close to the baseline. The off-diagonal cross-peaks, labeled A–G, indicate spin–spin coupling between protons on adjacent carbon atoms. The connectivities corresponding to each acyl chain cross-peak (A–G) are shown in Fig. 3 Full analysis of 2D L-COSY, is best observed in Fig. 4 where the pertinent areas have been expanded. Here it can be clearly seen that each lipid molecule resonates at two different frequencies consistent with the presence of an intra and extra cellular environment. The dispersion in Fig. 4 allowed for full discrimination between resonances arising from intra and extra cellular environment.

Cross-peaks, denoted A, E, F, G, and G′ are common to all triglyceride and diglyceride molecules [14]. Two diagonal peaks, consistent with carnosine, are seen at F2 = F1 = 7.1 ppm and 8.0 ppm.

Table 1
Assignment of resonances in the 1D MR spectrum of human soleus muscle collected *in vivo* at 7T shown in Fig. 1.

Molecules	Peak	Species	Chemical shift (ppm)
Intra-myocellular lipids	1	**CH$_3$**	0.84
Extra-myocellular lipids	2	**CH$_3$**	1.05
Intra-myocellular lipids	3	(**CH$_2$**)*n*	1.25
Extra-myocellular lipids	4	(**CH$_2$**)*n*	1.44
Intra-myocellular lipids	5	–**CH$_2$**–CH=CH–	2.00
Extra-myocellular lipids	6	–**CH$_2$**–CH=CH–	2.20
Intra-myocellular lipids	6	–**CH$_2$**–(C=O)–OR	2.20
Extra-myocellular lipids	7	–**CH$_2$**–(C=O)–OR	2.43
Intra-myocellular lipids	8	–CH=CH–**CH$_2$**–CH=CH–	2.76
Extra-myocellular lipids	9	–CH=CH–**CH$_2$**–CH=CH–	2.93
Total creatine	10	**CH$_3$**	3.02*
Carnitine/choline	11	N(**CH$_3$**)$_3$	3.18
Taurine	12″	H_2N–CH_2–**CH_2**–SO_3	3.41
Pcho, Cho, GPC	12′	$(CH_3)_3$–N–**CH_2**–CH_2–OPO_3	3.63
Total creatine	12	**CH$_2$** (tCr)	3.92
Residual water	13	H_2O	4.70
Total lipid	14	–**HC**=C**H**–, –(C=O)–O–C**H**R_2	5.55

* Cr methyl peak at 3.02 ppm was used as a chemical shift reference.

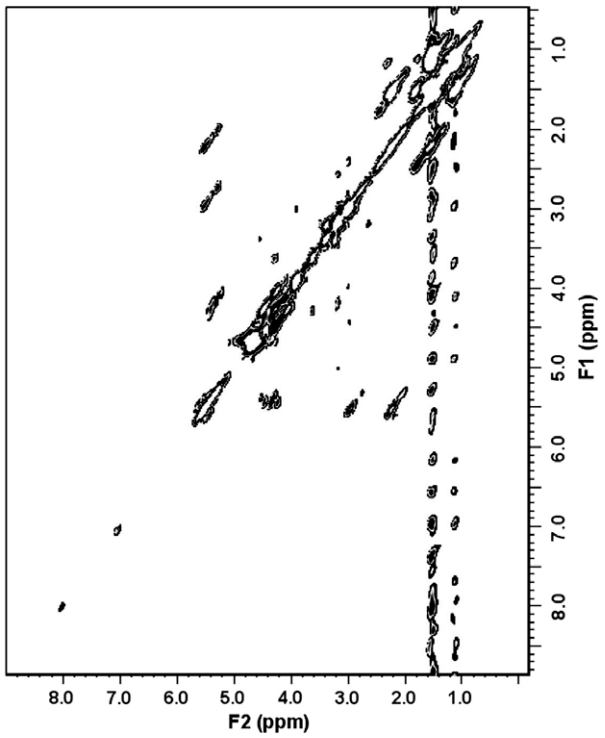

Fig. 2. 7T 2D localized ^{1}H L-COSY spectrum of human soleus muscle *in vivo*. See acquisition and processing parameters in text. Voxel position as shown in Fig. 1.

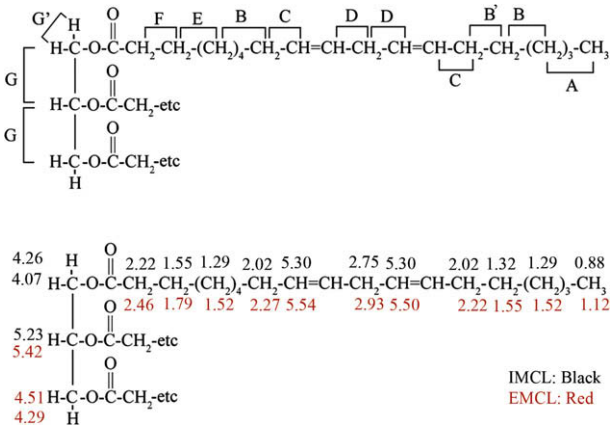

Fig. 3. Structures of the triglyceride molecule with the connectivities corresponding to each acyl chain cross-peak (A–F) as shown in Figs. 2 and 3. Cross-peaks, denoted A, E, F, G, and G′ are common to all triglyceride and diglyceride molecules. Resonance nomenclature according to [10]. Top: triglyceride molecule with the connectivities corresponding to each lipid cross-peak as shown in Figs. 2 and 3. Cross-peaks, denoted A, B, B′, C, D, E, F, G, and G′ are common to all triglyceride and diglyceride molecules. Bottom: chemical shifts values in IMCL in black color and EMCL in red color as derived from 2D L-COSY studies as shown in Fig. 2. Note the increase of 0.20–0.26 ppm for all EMCL moieties relative to IMCL. (For interpretation of the references to colour in this figure legend, the reader is referred to the web version of this article.)

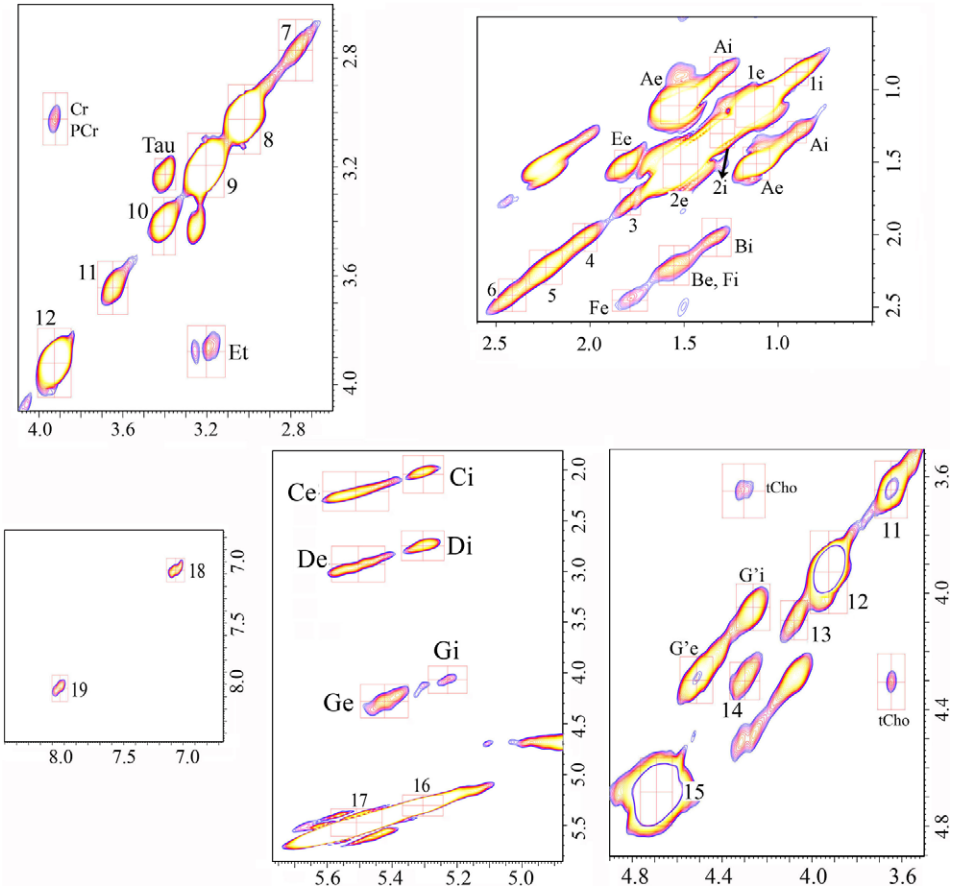

Fig. 4. 7T 2D localized ^{1}H L-COSY of human soleus muscle (data collected from voxel shown in Fig. 1). See Table 2 for assignments. Expansions reveal details in crowded spectral regions. The tCr methyl resonance at 3.02 ppm was used as an internal chemical shift reference. Horizontal (F2) and vertical (F1) axes have ppm units.

No residual dipolar coupling for carnosine was detected in all cases. Resonances observed in the muscle 2D spectrum were assigned and listed in Table 2.

Only when adequate shimming was achieved (magnitude line width at half height of the unsuppressed water of 40 Hz or less), the creatine (Cr) methylene group was seen as a doublet in the 1D spectrum with the separation varying between 10 and 20 Hz. With the spectral dispersion available in these experimental conditions, cross-peaks Ci, Ce, Di and De can be used to determine the level of unsaturation in the lipid molecules by measuring the ratios of cross-peaks Di/Ci (intra-myocellular = 1.13 ± 0.14) and De/Ce (extra-myocellular = 0.72 ± 0.11), which are consistent with literature values [21]. Also, using the 1.3(IMCL $(CH_2)_n$), 1.5(EMCL $(CH_2)_n$), and 3.02 (tCr CH_3) ppm diagonal resonances from the L-COSY experiments, the IMCL/tCr and EMCL/tCr were calculated and found to be 5.4 ± 2.4 and 19.2 ± 4.7, respectively.

T1 and T2 weighted spectra acquired from human soleus muscle *in vivo* at 7T are shown in Fig. 5. T1 and T2 values of detected resonances with their assignments are shown in Table 3. The 1D resonances were assigned as in [14,19,20]. T1 and T2 values of many resonances that were not reported previously are shown in Table 3. Water T1 and T2 data failed to fit to a bi-exponential model upon data analysis.

4. Discussion

4.1. 2D L-COSY

Two-Dimensional L-COSY techniques provide spectral dispersion that is not available with one-dimensional methods. Even though the 1D spectrum was acquired and assigned (Fig. 1 and Table 1), many peaks still overlap even at a field of 7T. For the first time, full assignments of all IMCL and EMCL molecular fragments are separated and assigned *in vivo* as shown in Fig. 4 and Table 2. In addition to the full IMCL and EMCL assignment, resonances due to ethanolamine, taurine, total creatine (tCr), carnosine, and total-choline (tCho) were identified and assigned. All cross-peaks from metabolites of interest were observed, except choline cross-peak (3.5,4.0) ppm which was difficult to observe in L-COSY spectrum, possibly due to the short T2 value of the methylene groups at 7T field strength. Cross-Peak Ei (–OOC–CH_2–C**H_2**–(CH_2)$_n$, IMCL) at (1.55,1.29) ppm was also not detected in most acquired 2D spectra.

The vertical ridge of noise (t1-noise) that appears at ~1.6 ppm in many L-COSY spectra was a nuisance, but did not compromise the spectral assignment. This is the regular and undesired t1-noise that riddled the early stage of high resolution 2D spectroscopy in the 70's. Few attempts were made to reduce this "t1-ridge" but were unsuccessful. Attempts were made to acquire the L-COSY matrix in an increasing Δt1 or decreasing Δt1 as suggested elsewhere [40], or by modifying the first point of matrix row [41], but results were not very encouraging. More work is needed in this field to improve the robustness of the technique.

Small changes between chemical shifts obtained from diagonal peaks and cross-peaks were observed in most *in vivo* 2D spectra. This is probably due to a combination of J-coupling effect and line broadening which might affect diagonal peaks and cross-peaks differently.

Cross-peaks due to IMCL (1.29,0.88) ppm and EMCL (1.52,1.12) ppm can be easily seen in Fig. 4. Cross-peaks do not only reflect on the relative amounts on IMCL and EMCL, but also confirm the

Table 2
Diagonal and cross-peaks assignment of soleus muscle L-COSY spectrum acquired at 7T field strength. L-COSY spectrum is shown in Figs. 2 and 4.

Molecules	Peak #	H–H coupling	Chemical shift (ppm) F2–F1
Lipid cross-peaks			
	Ai	$-(CH_2)_n-\mathbf{CH_2}-\mathbf{CH_3}$ (IMCL)	1.29–0.88
	Ae	$-(CH_2)_n-\mathbf{CH_2}-\mathbf{CH_3}$ (EMCL)	1.52–1.12
	Ee	$-OOC-CH_2-\mathbf{CH_2}-(\mathbf{CH_2})_n-$ (EMCL)	1.81–1.52
	B′i	$-CH{=}CH-\mathbf{CH_2}-\mathbf{CH_2}-(CH_2)_n-$ (IMCL)	1.32–2.02
	Fi, B′e	$-OOC-\mathbf{CH_2}-\mathbf{CH_2}-(CH_2)_n-$(IMCL), $-CH{=}CH-\mathbf{CH_2}-\mathbf{CH_2}-$ (EMCL)	1.55–2.22
	Fe	$-OOC-\mathbf{CH_2}-\mathbf{CH_2}-(CH_2)_n-$ (EMCL)	1.79–2.46
	G′i	R–(CO)–O–$\mathbf{CH'H''}$–CH–O–(CO)–R (IMCL)	4.26–4.05
	G′e	R–(CO)–O–$\mathbf{CH'H''}$–CH–O–(CO)–R (EMCL)	4.51–4.29
	Ce	$-CH_2-\mathbf{CH_2}-\mathbf{CH}{=}CH$ (EMCL)	5.54–2.27
	Ci	$-CH_2-\mathbf{CH_2}-\mathbf{CH}{=}CH$ (IMCL)	5.30–2.02
	De	$-CH{=}\mathbf{CH}-CH_2-\mathbf{CH}{=}CH$ (EMCL)	5.50–2.93
	Di	$-CH{=}\mathbf{CH}-\mathbf{CH_2}-\mathbf{CH}{=}CH-$ (IMCL)	5.30–2.75
	Ge	$-\mathbf{CH}-\mathbf{CH_2}-OCO-$ (glycerol backbone, EMCL)	5.42–4.29
	Gi	$-\mathbf{CH}-\mathbf{CH_2}-OCO-$ (glycerol backbone, IMCL)	5.23–4.07
Lipid diagonal peaks			
	1e	$-(CH_2)_n-CH_2-\mathbf{CH_3}$ (EMCL)	1.12–1.12
	2e	$-(\mathbf{CH_2})_n-CH_3$ (EMCL)	1.52–1.52
	1i	$-(CH_2)_n-CH_2-\mathbf{CH_3}$ (IMCL)	0.90–0.89
	2i	$-(\mathbf{CH_2})_n-CH_3$ (IMCL)	1.30–1.31
	3	$-OOC-CH_2-\mathbf{CH_2}-$ (EMCL)	1.78–1.78
	4	$-CH{=}CH-\mathbf{CH_2}-CH_2-$ (IMCL)	2.03–2.03
	5	$-OOC-\mathbf{CH_2}-$(IMCL), $-CH{=}CH-\mathbf{CH_2}-CH_2-$ (EMCL)	2.23–2.23
	6	$-OOC-\mathbf{CH_2}-$ (EMCL)	2.41–2.42
	7	$-CH{=}CH-\mathbf{CH_2}-CH{=}CH-$ (IMCL)	2.77–2.77
	13	R–(CO)–O–CH′$\mathbf{H''}$–CH–O–(CO)–R	4.06–4.06
	14	R–(CO)–O–$\mathbf{CH'}$H″–CH–O–(CO)–R	4.30–4.30
	16	$-\mathbf{CH}{=}\mathbf{CH}-$ (IMCL)	5.30–5.30
	17	$-\mathbf{CH}{=}\mathbf{CH}-$ (EMCL)	5.54–5.54
Metabolites cross-peaks			
Ethanolamine	Et	$H_3N^+-\mathbf{CH_2}-\mathbf{CH_2}-OH$	3.15–3.87
Taurine	Tau	$H_2N-\mathbf{CH_2}-\mathbf{CH_2}-SO_3$	3.40–3.23
Creatine/PhCr	Cr, PCr	$-(\mathbf{CH_3})N-\mathbf{CH_2}-CO_2$	3.02–3.92
Cho, PCho, GPC	tCho	$(CH_3)_3-N-\mathbf{CH_2}-\mathbf{CH_2}-OPO_3$	3.65–4.31
Metabolites diagonal peaks			
Cr/PhCr*	8	$R-N-\mathbf{CH_3}$	3.02–3.02
Cho, taurine	9	$-(\mathbf{CH_3})_3-N-CH_2-CH_2-OH$, $H_2N-\mathbf{CH_2}-CH_2-SO_3$	3.20–3.20
Taurine	10	$H_2N-CH_2-\mathbf{CH_2}-SO_3$	3.40–3.40
PCho, Cho, GPC	11	$(CH_3)_3-N-\mathbf{CH_2}-CH_2-OPO_3$	3.65–3.65
Creatine/PhCr	12	$RN-\mathbf{CH_2}-CO_2$	3.92–3.93
PCho, GPC	14	$(CH_3)_3-N^+-CH_2-\mathbf{CH_2}-OPO_3$	4.31–4.31
H_2O	15	H_2O	4.69–4.69
Carnosine	18	$RNH-\mathbf{CH}{=}CR_2$	7.07–7.07
Carnosine	19	$RNH-\mathbf{CH}{=}NR$	8.05–8.05

'i' and 'e' in table stand for IMCL and EMCL, respectively.
* Cr methyl peak at 3.02 ppm was used as a chemical shift reference.

identity of the molecular fragments from which these peaks arise. However, the dispersion along the diagonal for $(CH_2)_n$ from IMCL and EMCL provides a more accurate measure of these compartments. Using the 2D L-COSY data, the IMCL/tCr and EMCL/tCr were found to be 5.4 ± 2.4 and 19.2 ± 4.7, respectively. These results are different from what was found earlier [21], but matches with male-only derived ratios reported elsewhere [27]. Velan et al. explored the use of 2D ^{1}H MRS for quantification of IMCL and EMCL at 3T [21]. However, even at 3T there is significant overlap of the resonances in the 1D and cross-peaks in the 2D MR spectra making assignment and definitive correlations with disease difficult.

It was reported that the total-choline (tCho) resonance to tCr resonance (tCho/tCr ratio) at 1.5T can vary from one muscle type to another in the same person and between healthy and diseased muscles [42]. The ratio of tCho/tCr, at 1.5T, was found to be 0.6 when recorded in a 1D spectrum with a TE of 30 ms. In the present study at 7T, the tCho/tCr ratio was found to be 1.15 ± 0.24 in L-COSY spectrum by comparing the diagonal peaks. A T1 increase and a T2 decrease of tCho and tCr is expected with Bo elevation [43], which might explain the higher tCho/tCr ratio obtained here. However, it is expected that this ratio to be Bo dependent.

It has been described by others that MR spectroscopy can provide information about the IMCL and EMCL in muscle and that the lipid resides in different compartments which causes their protons to be shielded differently [20]. Researchers [19,44] suggested that EMCL is located in long fatty septa along the muscle fiber bundles or fasciae, whereas IMCL are within the cytoplasm of muscle cells as spherical droplets. At 1.5T, this resulted in a chemical shift separation of 0.2 ppm between the two compartments in the tibialis anterior and 0.15 ppm in the soleus compartment [19,44]. These chemical shift differences were observed for methyl and methylene resonances arising from the IMCL and EMCL. Here, we confirm the chemical shift separation range of 0.20–0.26 ppm between *all* the resonances of the EMCL and IMCL moieties in the soleus muscle from spectra collected at 7T. Note that IMCL and EMCL resonance frequencies are different for every set of protons within the lipid molecule with an increase ranging from 0.20 to 0.26 ppm for EMCL groups relative to the IMCL groups (Fig. 3). The difference between chemical shifts between the IMCL/EMCL has been associated with bulk magnetic susceptibility (BMS) which describes the extent that the material increases or decreases the applied magnetic field [44]. This variation in BMS between different materials

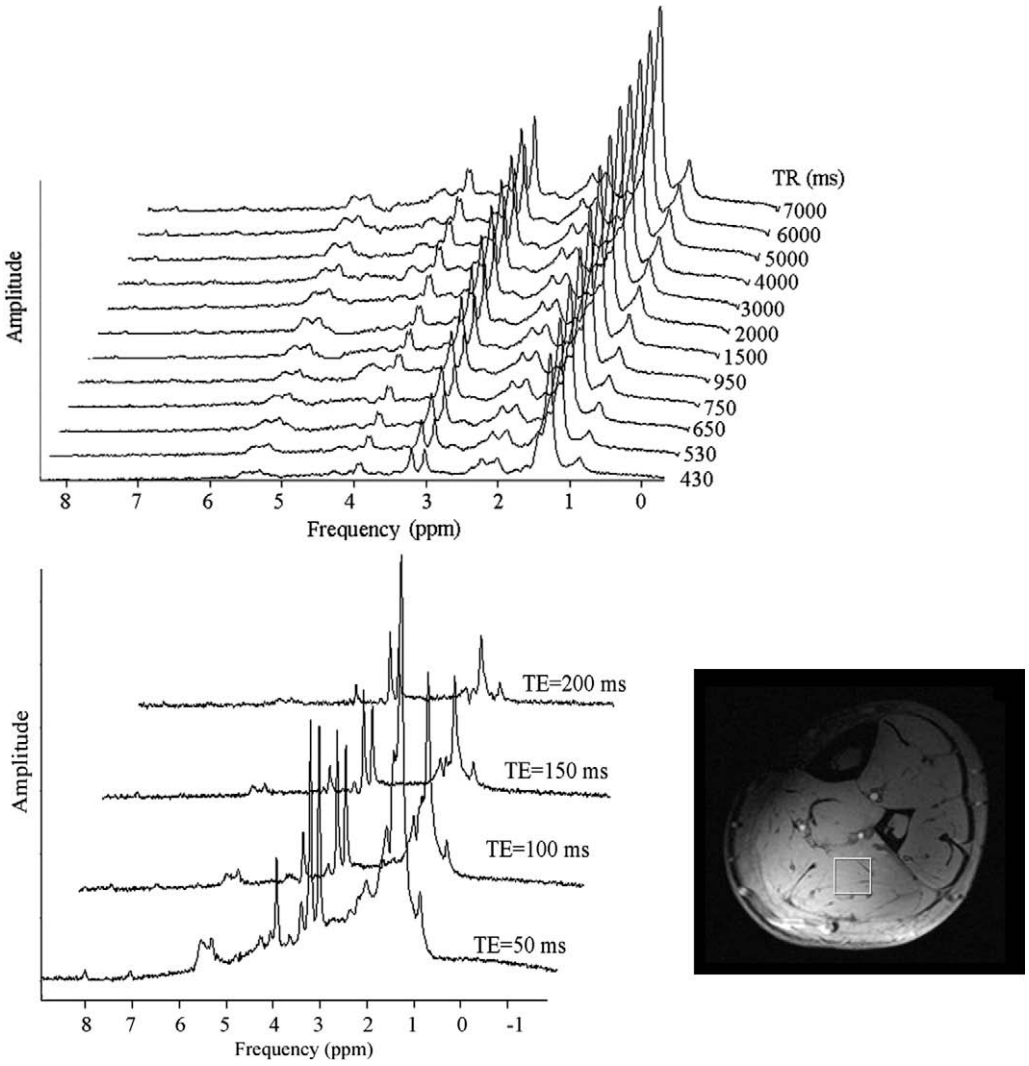

Fig. 5. Representative T1 (above) and T2 (below) array of spectra acquired from a healthy volunteer. The creatine methyl peak at 3.02 ppm was used as an internal chemical shift reference.

(as a result of experiencing a different 'apparent' magnetic field) introduces an additional frequency shift to the standard resonance (Larmor) frequency.

IMCL are known to be liquid and spherical droplets where as EMCL are portrayed as nearly cylindrical clusters of lipids aligned between muscle fibers. The symmetrical spherical shape of IMCL means that its BMS frequency shift contribution is negligible compared to that of EMCL fibers that might be orthogonal to or aligned with the applied magnetic field [45]. That is the main reason why IMCL resonances do not vary, while those of EMCL do, when the orientation of muscle fiber in a magnetic field is varied. BMS seems to affect different fragments of the lipid molecule differently. This differential intramolecular behavior of BMS is not unexpected due to the effect of chemical shielding, vis-à-vis chemical shift, on magnetic susceptibility.

The improved spectral resolution at 7T combined with the 2D spectroscopy method offers a new opportunity for inspection of lipid alterations in muscle associated with a range of diseases. Two potential examples of this include the effect of the cholesterol-lowering drugs, statins that commonly cause muscle pain or weakness and can progress to rhabdomyolysis and mortality [46]. Another is the relationship between skeletal muscle triglycerides and insulin resistance, obesity and exercise [47].

4.2. Relaxation measurements

Stimulated echo spectroscopy was preferred to double echo, even though the latter gives higher signal-to-noise ratio per unit time, due to the claim that anomalous J-coupling behavior in double echo sequences might interfere with measurements of T1 and T2 values [48,49].

T1 and T2 constants of IMCL are expected to be longer than their EMCL counterparts, due to the isotropic nature of the IMCL present in the spherical droplets in contrast to dense and oriented EMCL present along the muscle fibers. This was observed at 3T [23] where T2 $(CH_2)_n$IMCL > T2 $(CH_2)_n$IMCL, but not at 7T [26] where T1 $(CH_2)_n$IMCL < T1 $(CH_2)_n$IMCL. In addition, T1 and T2 values of the lipid CH_3 groups are expected to be longer than T1 and T2 values of $(CH_2)_n$, due to the efficient relaxation mechanisms available for the $(CH_2)_n$ group. Relaxation times constants obtained in this work are listed in Table 3. Comparison of relaxation time constants with respect to each other in Table 1 reveals that they have met the above expectations.

A resonance at 2.4 ppm was assigned to COC**H$_2$**CH=CH in Wang et al. [26]. Careful inspection of the lipid structural formula shown in Fig. 3 reveals that such a fragment (COC**H$_2$**CH=CH) does not exist. A better assignment seems to be the –O–CC**H$_2$** fragment in the

Table 3
T1 and T2 relaxation values of resonances from human soleus muscle *in vivo* at 7T. The standard deviation is shown in brackets.

Chemical shift (ppm)	Species	T1(SD) ms	T2(SD) ms
0.88	C**H**$_3$ (IMCL)	1735(132)	85(23)
1.12	C**H**$_3$ (EMCL)	1470(102)	117(28)
1.32	(C**H**$_2$)$_n$ (IMCL)	1350(193)	78(12)
1.51	(C**H**$_2$)$_n$ (EMCL)	1031(166)	64(10)
1.79	–O–CO–CH$_2$–C**H**$_2$	1343 (173)	65(9)
2.02	HC=CH–C**H**$_2$–	972(170)	36(5)
2.21	–OOC–C**H**$_2$– (IMCL)	1420(130)	49(10)
2.42	–OOC–C**H**$_2$– (EMCL)	907(206)	52(13)
3.02*	tCr(C**H**$_3$)	1320(121)	101(29)
3.20	tCho	1216(85)	93(18)
3.40	H$_3$N–CH$_2$–C**H**$_2$–SO$_3$ (taurine)	1573(181)	75(25)
3.65	–C**H**$_2$–CH$_2$–OPO$_3$ (PCho)	2244(440)	61(13)
3.91	Cr(C**H**$_2$)	1150(123)	74(8)
4.06	–CH**H**–O–CO (glycerol)	2031(534)	66(9)
4.26	–CH$_2$–C**H**$_2$–OPO$_3$ (PCho), –C**H**H–O–CO (glycerol)	1053(90)	47(8)
4.70	H$_2$O	1514(10)	22(2)
5.30	HC=CH (IMCL), HCO (glycerol)	1195(122)	72(19)
5.51	HC=CH (EMCL)	1398(190)	70(22)
7.05	Carnosine	908(165)	59(18)
8.01	Carnosine	1464(210)	86(19)

* Cr methyl 3.02 ppm was used as a chemical shift reference.

EMCL compartment, especially when taken with the 2.21 ppm resonance which can be assigned to the same fragment in the IMCL compartment. Relaxation measurements in Table 3 also support this assignment.

Carnosine concentration, as estimated from diagonal peak volume, was variable between different volunteers. Carnosine diagonal peaks can be seen in Fig. 4. T2 value of the 8.0 ppm peak of carnosine in soleus muscle *in vivo* at 3T was found to be 107.54 ± 25.34 [50]. Relaxation parameters for carnosine at 7T field strength have not been reported before. T2 value for the 8.0 ppm of carnosine at 7T was found to be 86 ± 19 ms, which is as expected less as the T2 value at 3T. T1 and T2 of carnosine are shown in Table 3.

T2 of water was determined by MRI studies to be 31 ms at 1.89T field strength in the flexor digitorum profundus (a deep muscle of the forearm that flexes the terminal phalanges of the four fingers) [51]. A more detailed study by the same authors [51] showed that at least four compartments of water exist with T2 values of 5, 21, 39 and 114 ms with variable fractional volumes. In the present study, the T2 weighted spectroscopic signal can only be fit to a mono-exponential curve, yielding a T2 value of 22 ± 2 ms.

5. Conclusions

The 2D L-COSY spectra, recorded at 7T from the soleus muscle, provide detailed information on metabolite ratios, lipid chemistry and multiple lipid compartments. For the first time, it is shown that all molecular moieties of IMCL and EMCL are 0.2 ppm shifted with respect to each other. At 7T the 2D method offers improved resolution and sensitivity compared with previous reports at 3 and 4T and the opportunity to study effect of disease in muscles. T1 and T2 relaxation constants were also determined and can be used to further improve spectroscopic sequence design.

Acknowledgments

This work was supported by a grant from the Australian Research Council Grant DP0663987 and NIH Grants R21NS059331 and R01NS050041. The MGH A.A. Martinos Center for Biomedical Imaging is also supported by National Center for Research Resources Grant No. P41RR14075 and the Mental Illness and Neuroscience Discovery (MIND) Institute.

References

[1] M. Goldman, M. Porneuf (Eds.), NMR and More in Honour of Anatole Abragam, vol. 112, Les Ulis Cedex A, France, 1994 (F-91944).
[2] J. Jeener, Ampere International Summer School, Basko Polje, Yugoslavia, 1971.
[3] K.J. Cross, K.T. Holmes, C.E. Mountford, P.E. Wright, Assignment of acyl chain resonances from membranes of mammalian cells by two-dimensional NMR methods, Biochemistry 23 (1984) 5895–5897.
[4] P.G. Williams, J.K. Saunders, M. Dyne, C.E. Mountford, K.T. Holmes, Application of a T2-filtered COSY experiment to identify the origin of slowly relaxing species in normal and malignant tissue, Magn. Reson. Med. 7 (1988) 463–471.
[5] C.E. Mountford, S. Doran, C.L. Lean, P. Russell, Proton MRS can determine the pathology of human cancers with a high level of accuracy, Chem. Rev. 104 (2004) 3677–3704.
[6] A.P. Chen, C.H. Cunningham, J. Kurhanewicz, et al., High-resolution 3D MR spectroscopic imaging of the prostate at 3 T with the MLEV-PRESS sequence, Magn. Reson. Imaging 24 (2006) 825–832.
[7] J. Kurhanewicz, M.G. Swanson, S.J. Nelson, D.B. Vigneron, Combined magnetic resonance imaging and spectroscopic imaging approach to molecular imaging of prostate cancer, J. Magn. Reson. Imaging 16 (2002) 451–463.
[8] D.A. Ende, C.L. Lean, W.B. Mackinnon, C.E. Mountford, P. Russell, Human colorectal adenoma–carcinoma sequence documented by ^{1}H MRS (ex vivo), Proc. Intl. Soc. Magn. Reson. Med. 2 (1993) 273.
[9] C.L. Lean, W.B. Mackinnon, E.J. Delikatny, R.H. Whitehead, C.E. Mountford, Cell-surface fucosylation and magnetic resonance spectroscopy characterization of human malignant colorectal cells, Biochemistry 31 (1992) 11095–11105.
[10] G.L. May, L.C. Wright, C.L. Lean, C.E. Mountford, Identification of 1-O-alkyl-2,3-diacyl-sn-glycerol in plasma membranes of cancer cells, J. Magn. Reson. 98 (1992) 622–627.
[11] C.L. Lean, W.B. Mackinnon, C.E. Mountford, Fucose in ^{1}H COSY spectra of plasma membrane fragments shed from human malignant colorectal cells, Magn. Reson. Med. 20 (1991) 306–311.
[12] G.L. May, K. Sztelma, T.C. Sorrell, C.E. Mountford, Comparison of human polymorphonuclear leukocytes from peripheral blood and purulent exudates by high resolution ^{1}H MRS, Magn. Reson. Med. 19 (1991) 191–198.
[13] G.L. May, L.C. Wright, M. Dyne, W.B. Mackinnon, R.M. Fox, C.E. Mountford, Plasma membrane lipid composition of vinblastine sensitive and resistant human leukaemic lymphoblasts, Int. J. Cancer 42 (1988) 728–733.
[14] G.L. May, L.C. Wright, K.T. Holmes, et al., Assignment of methylene proton resonances in NMR spectra of embryonic and transformed cells to plasma membrane triglyceride, J. Biol. Chem. 261 (1986) 3048–3053.
[15] E.J. Delikatny, W.E. Hull, C.E. Mountford, The effect of altering time domains and window functions in two-dimensional proton COSY spectra of biological specimens, J. Magn. Reson. 94 (1991) 563–573.
[16] I.M. Brereton, G.J. Galloway, S.E. Rose, D.M. Doddrell, Localized two-dimensional shift correlated spectroscopy in humans at 2 Tesla, Magn. Reson. Med. 32 (1994) 251–257.
[17] M.A. Thomas, N. Hattori, M. Umeda, T. Sawada, S. Naruse, Evaluation of two-dimensional L-COSY and JPRESS using a 3T MRI scanner: from phantoms to human brain in vivo, NMR Biomed. 16 (2003) 245–251.
[18] M.A. Thomas, K. Yue, N. Binesh, et al., Localized two-dimensional shift correlated MR spectroscopy of human brain, Magn. Reson. Med. 46 (2001) 58–67.
[19] C. Boesch, J. Slotboom, H. Hoppeler, R. Kreis, In vivo determination of intramyocellular lipids in human muscle by means of localized ^{1}H-MR spectroscopy, Magn. Reson. Med. 37 (1997) 484–493.
[20] F. Schick, B. Eismann, W.I. Jung, H. Bongers, M. Bunse, O. Lutz, Comparison of localized proton NMR signals of skeletal muscle and fat tissue in vivo: two lipid compartments in muscle tissue, Magn. Reson. Med. 29 (1993) 158–167.
[21] S.S. Velan, C. Durst, S.K. Lemieux, et al., Investigation of muscle lipid metabolism by localized one- and two-dimensional MRS techniques using a clinical 3T MRI/MRS scanner, J. Magn. Reson. Imaging 25 (2007) 192–199.
[22] S.S. Velan, S. Ramamurthy, S. Ainala, et al., Implementation and validation of localized constant-time correlated spectroscopy (LCTCOSY) on a clinical 3T MRI scanner for investigation of muscle metabolism, J. Magn. Reson. Imaging 26 (2007) 410–417.
[23] M. Krssak, V. Mlynarik, M. Meyerspeer, E. Moser, M. Roden, ^{1}H NMR relaxation times of skeletal muscle metabolites at 3T, Magn. Reson. Mater. Phys. Biol. Med. 16 (2004) 155–159.
[24] P.A. Bottomley, T.H. Foster, R.E. Argersinger, L.M. Pfeifer, A review of normal tissue hydrogen NMR relaxation times and relaxation mechanisms from 1–100 MHz: dependence on tissue type, NMR frequency, temperature, species, excision, and age, Med. Phys. 11 (1984) 425–448.
[25] J.H. Hwang, J.W. Pan, S. Heydari, H.P. Hetherington, D.T. Stein, Regional differences in intramyocellular lipids in humans observed by in vivo H-1-MR spectroscopic imaging, J. Appl. Physiol. 90 (2001) 1267–1274.
[26] L. Wang, N. Salibi, Y. Wu, M.E. Schweitzer, R.R. Regatte, Relaxation times of skeletal muscle metabolites at 7T, J. Magn. Reson. Imaging 29 (2009) 1457–1464.
[27] S. Velan, N. Said, K. Narasimhan, et al., Gender differences in musculoskeletal lipid metabolism as assessed by localized two-dimensional correlation spectroscopy, Magn. Reson. Insights 2 (2008) 1–6.

[28] H.T. Zandt, D.W.J. Klomp, F. Oerlemans, B. Wieringa, C.W. Hilbers, A. Heerschap, MR proton spectroscopy of wild-type, creatine kinase deficient mouse skeletal muscle: dipole–dipole coupling effects and post-mortem changes, Magn. Reson. Med. 43 (2000) 517–524.
[29] R. Freeman, H.D.W. Hill, Fourier transform study of NMR spin–lattice relaxation by "Progressive Saturation", J. Chem. Phys. 54 (1971) 3367–3377.
[30] K. Kamada, K. Houkin, K. Hida, et al., Localized proton spectroscopy of focal brain pathology in humans: significant effects of edema on spin–spin relaxation time, Magn. Reson. Med. 31 (1994) 537–540.
[31] A. Schwarcz, Z. Berente, E. Osz, T. Doczi, Fast in vivo water quantification in rat brain oedema based on T1 measurement at high magnetic field, Acta Neurochirurgica 144 (2002) 811–816.
[32] J. Knight-Scott, S.J. Li, Effect of long TE on T1 measurement in STEAM progressive saturation experiment, J. Magn. Reson. 126 (1997) 266–269.
[33] J. Frahm, H. Bruhn, M.L. Gyngell, K.D. Merboldt, W. Hanicke, R. Sauter, Localized high-resolution proton NMR spectroscopy using stimulated echoes: initial applications to human brain in vivo, Magn. Reson. Med. 9 (1989) 79–93.
[34] J. Frahm, K. Merboldt, W. Hanicke, Localized proton spectroscopy using stimulated echoes, J. Magn. Reson. 72 (1987) 502–508.
[35] R.J. Ogg, P.B. Kingsley, J.S. Taylor, WET, a T1- and B1-insensitive water-suppression method for in vivo localized ^{1}H NMR spectroscopy, J. Magn. Reson. Ser. B 104 (1994) 1–10.
[36] A. Naressi, C. Couturier, J.M. Devos, et al., Java-based graphical user interface for the MRUI quantitation package, Magn. Reson. Mater. Phys. 12 (2001) 141–152.
[37] S. Wolfram, The Mathematica Handbook, University Press, Cambridge, 2007.
[38] Felix, Felix NMR, Version 2007.
[39] S. Ramadan, E.M. Ratai, L.L. Wald, G.C. Wiggins, C.E. Mountford, 1D and 2D Correlation spectroscopy of muscle at 7T, in: Proc. Intl. Soc. Magn. Reson. Med., Toronto, Canada, 2008, p. 1569.
[40] A.F. Mehlkopf, D. Korbee, T.A. Tiggelman, R. Freeman, Sources of t1 noise in two-dimensional NMR, J. Magn. Reson. 58 (1984) 315–323.
[41] G. Otting, H. Widmer, G. Wagner, K. Wüthrich, Origin of t1 and t2 ridges in 2D NMR spectra and procedures for suppression, J. Magn. Reson. 66 (1986) 187–193.
[42] J. Hu, Y. Xia, Y. Shen, et al., Significant differences in proton trimethyl ammonium signals between human gastrocnemius and soleus muscle, J. Magn. Reson. Imaging 19 (2004) 617–622.
[43] R. Kreis, M. Koster, M. Kamber, H. Hoppeler, C. Boesch, In vivo spectroscopy at the magic angle and creatine supplementation for the elucidation of ^{1}H-MR spectra of human muscle, in: Proc. Intl. Soc. Magn. Reson. Med., Nice, France, 1995, p. 430.
[44] G. Steidle, J. Machann, C.D. Claussen, F. Schick, Separation of intra- and extramyocellular lipid signals in proton MR spectra by determination of their magnetic field distribution, J. Magn. Reson. 154 (2002) 228–235.
[45] L.S. Szczepaniak, R.L. Dobbins, D.T. Stein, J.D. McGarry, Bulk magnetic susceptibility effects on the assessment of intra- and extramyocellular lipids in vivo, Magn. Reson. Med. 47 (2002) 607–610.
[46] P.D. Thompson, P. Clarkson, R.H. Karas, Statin-associated myopathy, JAMA 289 (2003) 1681–1690.
[47] J. Machann, H. Haring, F. Schick, M. Stumvoll, Intramyocellular lipids and insulin resistance, Diabetes Obes. Metab. 2004 (2004) 239–248.
[48] R.A. de Graaf, In vivo NMR Spectroscopy: Principles and Techniques, Wiley, Chichester, New York, 1998, pp. 113–125.
[49] R.A. de Graaf, D.L. Rothman, In vivo detection and quantification of scalar coupled ^{1}H NMR resonances, Conc. Magn. Reson. 13 (2001) 32–76.
[50] M.S.R. Ozdemir, H. Reyngoudt, Y. De Deene, et al., Absolute quantification of carnosine in human calf muscle by proton magnetic resonance spectroscopy, Phys. Med. Biol. 52 (2007) 6781–6794.
[51] G. Saab, R.T. Thompson, G.D. Marsh, Multicomponent T2 relaxation of in vivo skeletal muscle, Magn. Reson. Med. 42 (1999) 150–157.
[52] MestReNova, Mestralab Research S.L., Version: 5.0.2-2108, 2007.